

MnO₂ MODIFIED LEAD LANTHANUM SILVER ZIRCONIUM TITANATE CERAMICS FOR DIELECTRIC AND PIEZOELECTRIC PROPERTIES

KODURI RAMAM[#], KEMBURU CHANDRAMOULI*

*Departamento de Ingeniería de Materiales, (DIMAT), Facultad de Ingeniería,
Universidad de Concepción, Concepción, Chile*

**Solid State Physics and Materials Research Laboratory, Department of Physics,
Andhra University, Visakhapatnam, India*

[#]Corresponding author, e-mail: ramamk@udec.cl

Submitted May 10, 2010; accepted November 1, 2010

Keywords: Ceramics; Microstructure; Dielectric properties; Piezoelectricity

This study highlights the influence of acceptors, Ag at A-site and Mn at B-site in $Pb_{(1-x-y)}La_xAg_y(Zr_zTi_{1-z})_{1-((x-y)/4)-(4k/4)}Mn_kO_3$ ceramic system where Mn (k) ranged from 0, 0.2, 0.4, 0.6, 0.8 and 1 mol% synthesized through solid state reaction method. Dielectric ($\epsilon_{RT} = 2802$) and piezoelectric properties ($d_{33} = 548$ pC/N, $k_p = 0.541$) were maximum at $Mn_{0.01}$ and can be attributed to (1) grain boundary kinetics via domain orientation with a reduction of oxygen vacancy migration, (2) compensation of lead vacancies by Mn and Ag, and (3) morphotrophic phase boundary shifting from coexistence of rhombohedral and tetragonal phase to tetragonality. The high electromechanical properties of this ceramic system were evaluated and are discussed with phase formation, microstructure, and dielectric characterization. It has been observed that the optimum properties are found in $Mn_{0.01}$ which could be suitable for possible energy harvesting or electromechanical applications.

INTRODUCTION

Lead zirconate titanate (PZT) compositions exhibit exceptionally high piezoelectric properties near the morphotrophic phase boundary (MPB) which separates ferroelectric tetragonal (FE_{TET}) and ferroelectric rhombohedral (FE_{RH}) phases and has been a major source for a wide range of applications such as sensors, actuators etc. It is known that the piezoelectric properties of Pb(Zr,Ti)O₃ solid solutions can be remarkably improved by compositional modifications [1]. The lead lanthanum zirconium titanate (PLZT) compounds with particular modifications, such as silver and manganese, also exhibit a large piezoelectric effect. Biggers and Schulze [2] have reported relatively high dielectric constant and low dissipation factor in Ag modified PLZT compositions.

Maher [3] noted that Ag⁺ dissolves in the PLZT (12/70/30) lattices as a large acceptor cation in the anti-ferroelectric region. PLZT with acceptor doping ions such as Fe [4-6], Mn [7-10] which occupy the B-site in the perovskite structure have also been investigated. Mn doped PZT [11-13] thin films prepared via the sol-gel technique were studied by Zhang et al [14]. Mn effect on multiple cations, [Pb_{0.961}La_{0.012}Ba_{0.015}Sr_{0.012}][Zr_{0.53}Ti_{0.47}]_{0.967-(h/2)}Nb_{0.02}Zn_{0.01}Mn_hO₃ (PLBSZZMNT)

nanoceramics for dielectric and piezoelectric properties had been studied [15]. Kanai et al have studied the effects of small amounts of silver doping in (Pb_{0.875}Ba_{0.125})(Mg_{1/3}Nb_{2/3})_{0.5}(Zn_{1/3}Nb_{2/3})_{0.3}Ti_{0.2}O₃ and have reported a decrease of the insulation resistance but an increase in the dielectric constant [16]. The changes are accompanied by an increase in density. The vacancy distribution in PLZT also influences the properties and the distribution of A-site and B-site vacancies in PLZT has been reported by Hardtl and Hennings [17]. PLZT ceramics have been modified with many acceptors like Mn [10], Ag [18] etc. However, there is no work reported on the influence of both the presence of acceptor Ag at A-site and Mn doping at B-site in [Pb,La][Zr_{0.527}Ti_{0.473}]O₃ system on dielectric and piezoelectric properties. Hence, we chose this study to find out the effect of Mn doping on the phase formation, microstructure, density, dielectric and piezoelectric properties in PLAZT solid solutions.

In this paper, we investigated the effect of acceptors Ag (A-site) and Mn (B-site) doping in PLZT solid solutions hereafter known as PLAZMT (Lead Lanthanum Silver Zirconium Manganese Titanate) on dielectric and piezoelectric properties. In relation to our previous systematic study of A-site and/or B-site modification with either donor and/or acceptor dopants

in PLZT solid solutions, we have been investigating the effect of dopant/s and their concentration with different Zr/Ti ratios on different properties. In this work, we have investigated the phase formation, microstructure, density, dielectric and piezoelectric properties of the PLAZMT solid solutions. The compositions synthesized and characterized are presented in Table 1.

around the samples to avoid PbO loss during sintering. After sintering, the samples were allowed to cool in the furnace. The detailed synthesis and characterization procedure has been stated elsewhere [6].

EXPERIMENTAL PROCEDURE

Synthesis

Analytical reagent grade powders (99.99 % purity) of PbO (Aldrich Chemicals Co. Inc., USA), La₂O₃ (Aldrich Chemicals Co. Inc., USA), Ag₂O (Wako Pure Chemical Co. Ltd., Japan) ZrO₂ (Kanto Chemicals Co. Inc., Tokyo, Japan), TiO₂ (Junsei Chemicals Co. Inc., USA) and MnO₂ (Aldrich Chemicals Co. Inc., USA) were used as starting raw materials and fabricated through solid state reaction method. Weighed components (as per stoichiometric ratios) were first wet mixed (zirconia balls and ethanol as media) for 24 h and calcined at 925°C for 3 h in alumina crucibles. Calcined powders were ball milled and mixed with 5 wt.% PVA binder and then pressed into pellets (of 12 mm diameter and 2 mm thickness) using steel die and hydraulic press with pressures of 68-100 MPa. The green bodies were sintered (with slow rate till 500°C to burn out binder) at 1225°C for 3 h in a closed alumina crucible in oxygen atmosphere. The PbO-rich atmosphere was maintained

Characterization

Phase formation, microstructural studies and apparent density

Sintered ceramics were characterized for apparent density by Archimedes method and phase formation with Philips X-ray diffractometer (PW-1710) using CuK_α radiation with Ni filter (scan rate of 1°/min and 2θ = 20 to 60°) at room temperature. Microstructural studies were carried out with scanning electron microscopy (SEM) of JEOL model JSM 840A for fractured surfaces. Grain sizes were measured by the linear interception method.

Dielectric and piezoelectric measurements

The lapped pellet surfaces were painted with silver paste and fired at 600°C for 1 h to form electrodes on sample surfaces. The dielectric constant (ε_{RT}), Curie temperature (T_c), dielectric maximum (ε_{Tc}) and tanδ of ceramics were characterized at 1 kHz using a 4192A HP Impedance Analyzer. The piezoelectric charge coefficients (d₃₃) of poled (silicon oil bath, 100°C, 20 kV/cm

Table 1. Mn modified PLAZT compositions

Composition	Formulae
General Formula	$Pb_{(1-x-y)}La_xAg_y(Zr_zTi_{1-z})_{1-((x-y)/4)-(4k/4)}Mn_kO_3$
Mol.%	x = La = 1.5, y = Ag = 0.5, z = Zr = 52.7, 1-z = Ti = 47.3, and k = Mn = 0, 0.2, 0.4, 0.6, 0.8 and 1 mol%, respectively.
PLAZMT	$[Pb_{0.98}La_{0.015}Ag_{0.005}][Zr_{0.527}Ti_{0.473}]_{0.9975-(4k/4)}Mn_kO_3$
0	$0.98PbO + 0.0075La_2O_3 + 0.0025Ag_2O + 0.5257ZrO_2 + 0.4718TiO_2 \rightarrow [Pb_{0.98}La_{0.015}Ag_{0.005}][Zr_{0.527}Ti_{0.473}]_{0.9975}O_3$
0.2	$0.98PbO + 0.0075La_2O_3 + 0.0025Ag_2O + 0.5246ZrO_2 + 0.4709TiO_2 + 0.002MnO_2 \rightarrow [Pb_{0.98}La_{0.015}Ag_{0.005}][Zr_{0.527}Ti_{0.473}]_{0.9955}Mn_{0.002}O_3$
0.4	$0.98PbO + 0.0075La_2O_3 + 0.0025Ag_2O + 0.5236ZrO_2 + 0.4699TiO_2 + 0.004MnO_2 \rightarrow [Pb_{0.98}La_{0.015}Ag_{0.005}][Zr_{0.527}Ti_{0.473}]_{0.9935}Mn_{0.004}O_3$
0.6	$0.98PbO + 0.0075La_2O_3 + 0.0025Ag_2O + 0.5225ZrO_2 + 0.4690TiO_2 + 0.006MnO_2 \rightarrow [Pb_{0.98}La_{0.015}Ag_{0.005}][Zr_{0.527}Ti_{0.473}]_{0.9915}Mn_{0.006}O_3$
0.8	$0.98PbO + 0.0075La_2O_3 + 0.0025Ag_2O + 0.5215ZrO_2 + 0.4680TiO_2 + 0.008MnO_2 \rightarrow [Pb_{0.98}La_{0.015}Ag_{0.005}][Zr_{0.527}Ti_{0.473}]_{0.9895}Mn_{0.008}O_3$
1.0	$0.98PbO + 0.0075La_2O_3 + 0.0025Ag_2O + 0.5204ZrO_2 + 0.4671TiO_2 + 0.01MnO_2 \rightarrow [Pb_{0.98}La_{0.015}Ag_{0.005}][Zr_{0.527}Ti_{0.473}]_{0.9875}Mn_{0.010}O_3$

* Decimal places have been limited to 4 significant digits

for 45 min, 24 h aging) PLAZMT ceramics were characterized using a Berlincourt piezo-d-meter. The k_p was characterized in accordance with the IRE standards on piezoelectric crystals and measurements of piezoelectric ceramics and the following formula has been employed:

$$\frac{k_p^2}{1-k_p^2} = 2.51 \times \left[\frac{f_a - f_r}{f_r} \right] \quad (1)$$

where, k_p = piezoelectric planar coupling coefficient, f_r = resonance frequency and f_a = anti-resonance frequency of poled ceramic. The resonance (f_r) and anti-resonance (f_a) frequencies were measured by using a 4192A HP impedance analyzer.

RESULTS AND DISCUSSION

XRD analysis, tolerance factor and electronegativity difference

Figure 1 shows the X-ray diffraction (XRD) patterns of PLAZMT ceramics. The peak splittings of (002) and (200), and (112) and (211) can be observed as the Mn (k in Figure 1) content increased to 1 mol.%. The ionic radii of the constituent compounds in this study are in accordance with the report on ionic radii by Shannon [19]. Owing to the similar ionic radii of Ag⁺ ($R_{Ag} = 1.28 \text{ \AA}$) and Pb²⁺ ($R_{Pb} = 1.49 \text{ \AA}$), the silver ions tend to occupy the A-site as acceptor in PLZT perovskite and also the cage site in the perovskite structure does not allow large B-site cations. Since, the ionic radii of La³⁺ ($R_{La} = 1.36 \text{ \AA}$) and Pb²⁺ ($R_{Pb} = 1.49 \text{ \AA}$) are also similar, the La³⁺ will tend to occupy A-site as donor. The similarity of the Mn⁴⁺ radius ($R_{Mn} = 0.53 \text{ \AA}$) to that of Zr⁴⁺ ($R_{Zr} = 0.72 \text{ \AA}$) and Ti⁴⁺ ($R_{Ti} = 0.605 \text{ \AA}$) results in Mn⁴⁺ occupying B-site

in (Pb²⁺, La³⁺, Ag⁺)(Zr⁴⁺, Mn⁴⁺, Ti⁴⁺)O₃ perovskite. Both La (donor) and Ag (acceptor) ions occupying the A-site partially substitute the Pb²⁺ and create cation vacancies at the B-site and Ag reduces the lead vacancies generated by La substitution, while Mn ions occupying B-site reduce the oxygen vacancy mobility by charge compensation in the PLZT perovskite. The chosen composition was near the MPB (Zr:Ti ratio = 52.7:47.3) where XRD patterns indicate coexistence (FE_{RH} and FE_{TET}) in the undoped composition (without Mn, $k = 0$) and the MPB shifted to (FE_{TET}) tetragonality as Mn content increased. It is considered that both Mn and Ag ions compensate the excess charge of the oxygen and lead vacancies in the perovskite lattice, respectively [20].

The perovskite structure is a network oxide with the general formula ABO₃, wherein the total of the sum of the average valences on the A and B cation sites is +6. In a perovskite structure, the cations on the A-site is 12-fold-coordinated octahedral site and is most readily occupied by large ions with crystal radii greater than or equal to that of O²⁻ (1.26 Å). The B-site is a 6-fold-coordinated octahedral site typically occupied by smaller ions [19]. In our study, the cations occupying the A-site are Pb²⁺, La³⁺, and Ag⁺, and the cations Zr⁴⁺, Ti⁴⁺, and Mn⁴⁺ occupy the B-site. The average A-site charge valence is 2 and the average B-site charge valence is 4. The charge valence state of the anion site is [O₃²⁻ = -6] and that of the cation site can be +6 and thus the sum is zero [i.e. (Pb²⁺, La³⁺, Ag⁺)(Zr⁴⁺, Ti⁴⁺)O₃ = 6+ (-6) = 0]. The charge balanced chemical equations of the ceramic compositions are given in Table 1. Hence, it can be justified that the multiple dopants substitute in the perovskite structure with perfect charge balance.

The formation of the perovskite between the A, B and O ions is given by the tolerance factor t . Goldschmidt had shown that the cubic perovskite is stable only if a tolerance factor t , defined by

$$t = \frac{r_A + r_O}{\sqrt{2}(r_B + r_O)} \quad (2)$$

lies in the approximate range of $0.8 < t < 0.99$ and a slightly larger range for distorted perovskite structures. The phase stability of the crystal structure can be determined by averaged electronegativity difference which is another important parameter. In addition to using the tolerance factor t to categorize the perovskite structure, the average electronegativity is expressed by

$$e = \frac{(\chi_A - \chi_O) + (\chi_B - \chi_O)}{2} \quad (3)$$

where χ_A , χ_B and χ_O are the individual electronegativities of the A and B site cations and the O²⁻ anion, respectively. By using the general formula for the complex material perovskite system, the averaged electronegativity difference e can be written as:

$$e = \{0.98\chi_{Pb-O} + 0.015\chi_{La-O} + 0.005\chi_{Ag-O} + [(0.9975 - (4k/4)) (0.527\chi_{Yr-O} + 0.473\chi_{Ti-O})] + k\chi_{Mn-O}\} - 1.9975 \quad (4)$$

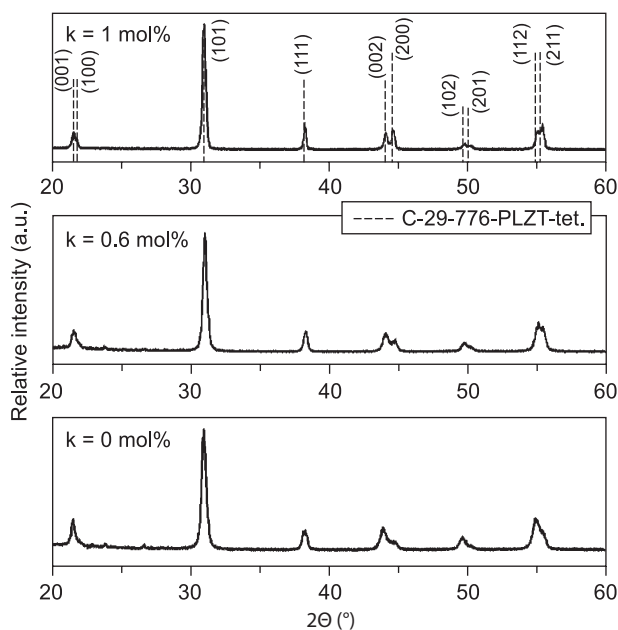


Figure 1. X-ray diffraction (XRD) patterns of PLAZMT ceramics.

The tolerance factor and averaged electronegativity difference are widely used to evaluate the stability of perovskite. The tolerance factor and averaged electronegativity difference have been calculated using the effective ionic radii [19] and revised Pauling's electronegativity, respectively. The tolerance factor versus the averaged electronegativity difference for all the compositions (refer Table 2) has shown that stability increases with both tolerance factor and averaged electronegativity difference. It has been observed that PLAZMT ceramic system has a stable tetragonal phase supported by the tolerance factor t and averaged electronegativity difference e .

density > 98% theoretical density. It is usual that at the MPB, the domain wall movement is rapid and depends on the intrinsic properties of the perovskite ceramic system [21]. Ag had exhibited different tendencies when used as an electrode and as a dopant [22]. The shift in the MPB is also an important contribution in relation to the enhancement of grain size. It is observed that small quantities of Mn reduce the mobility of oxygen vacancies

Microstructural and apparent density studies

Figure 2 shows the average grain size and apparent density for undoped and Mn modified PLAZT ceramics. Figure 3 shows scanning electron micrographs of 0.8 and 1 mol% Mn modified PLAZT fractured ceramics. As can be seen from the Figure 2 the grain size increases as Mn content increases. The sintered ceramics had an apparent

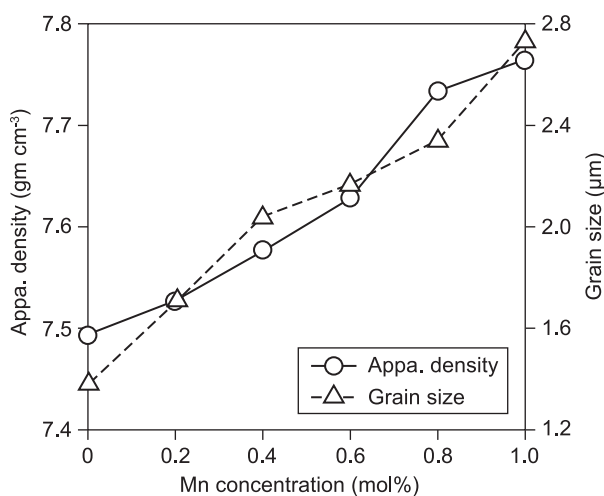
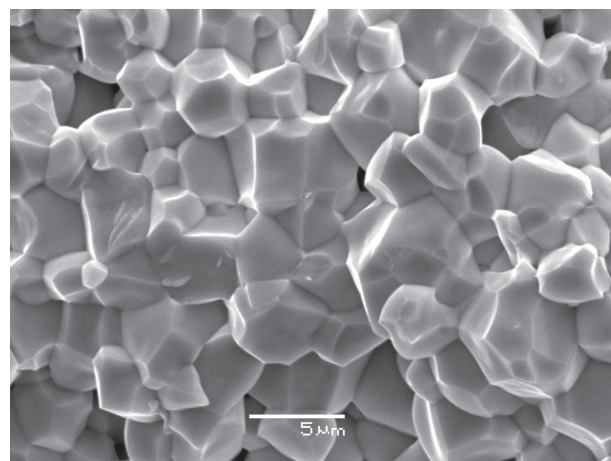
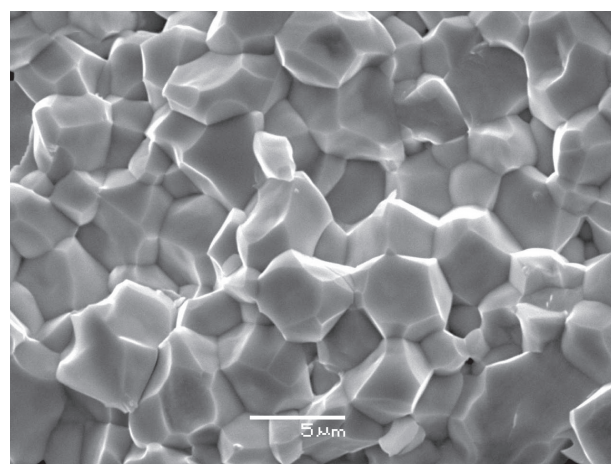


Figure 2. Grain size and apparent density of PLAZMT ceramics.



a) 0.8 mol% Mn



b) 1 mol% Mn

Figure 3. Scanning electron micrographs of 0.8 and 1 mol.% Mn modified PLAZT fractured ceramics, respectively.

Table 2. Tolerance factor t and electronegativity difference e .

Cations	Fold Coord No.	Paulings Electroneg. diff. e	Ionic radii (Å)	Mn (mol. %)	Tolerance factor t	Electronegativity difference e
Pb ²⁺	12	2.33	1.49	0	0.9891	1.5700
La ³⁺	12	1.10	1.36	0.2	0.9892	1.5698
Ag ⁺	8	1.93	1.28	0.4	0.9893	1.5696
Zr ⁴⁺	6	1.33	0.72	0.6	0.9894	1.5695
Ti ⁴⁺	6	1.54	0.605	0.8	0.9896	1.5693
Mn ⁴⁺	6	1.55	0.53	1	0.9897	1.5691
O ⁶⁺	6	3.44	1.4	—	—	—

and therefore, reduce the concentration of domain-stabilizing defect pairs, while Ag tends to balance the vacancies caused by La resulting in homogeneous distribution in the PLZT perovskite structure. The vacancy distribution depends on two factors (1) PbO partial pressure during sintering and (2) Zr/Ti ratio. It is assumed that due to the coexistence of vacancies both at A-site and B-site which compensates each other, the densification of the ceramics is promoted. Another mechanism for increase in density could be due to the distribution of Ag in the lattice as an acceptor cation which tends to charge compensate for the La³⁺ donor ions. It has been reported that the density increased rapidly due to the formation of lattice vacancies by the diffusion of Mn [23]. It is evident that additives can also enhance densification kinetics via defect structures due to Mn and compensation of lead vacancies due to Ag. According to literature, the effect of PbO content on densification kinetics has been reported [24, 25]. In our study, the microstructure evolution and homogeneous grain growth helped in increasing the density of the PLAZMT ceramics.

Dielectric behavior

Figure 4 shows dielectric properties, room temperature dielectric constant (ϵ_{RT}), dielectric maximum (ϵ_{TC}) and Curie temperature (T_c) vs. grain size of PLAZMT ceramics, respectively. With respect to the variation of ϵ_{RT} as a function of Mn concentration, the dielectric constant increases with increasing Mn and reaches a maximum for Mn_{0.01} or $k = 1$ mol%. It is well known that the presence of domain-walls and their movement contribute considerably to the dielectric, piezoelectric and elastic properties of the PZT ceramics [26]. Figure 2 shows that as the grain size increases, the dielectric constant significantly increases, while Curie temperature decreases continuously. The addition of Mn in PLAZT improved the dielectric constant, and with 1 mol.% Mn a dielectric constant of 2802 was obtained. The Curie temperature, T_c (from 298°C to 207°C) continuously decreased. The dielectric loss ($\tan\delta_{RT}$) decreased from 0.0534 (undoped) to 0.0382 (1 mol.% Mn). The addition of Ag and Mn (acceptors) seem to enhance crystallization and moves the structural phase towards tetragonal. The increase in tetragonality and grain growth at or near MPB results in increased dielectric constant. The dielectric behavior may be attributed to the increase of concentration of lead vacancies interacting with mobile domain boundaries and/or due to the oxygen vacancies electrostatically interacting with pinned domain walls. The enhanced dielectric constant may be attributed to tetragonality and increased grain growth with reduced concentration of oxygen vacancies being trapped by Mn content or in other words Mn restricts the oxygen vacancy migration to charge balance in PLAZMT ceramics [27, 28].

Piezoelectric properties

Figure 5 shows d_{33} and k_p of undoped and Mn modified PLAZT ceramics. In this study, piezoelectric properties of ceramics increase approximately linearly with increasing Mn concentration and grain size. The piezoelectric coefficients enhanced due to the increasing polarization which could be attributed to the movement of the domain walls, and microstructural evolution is associated with the perovskite phase. Figure 2 also shows the density variation and it is evident that dense PLAZT ceramics would have better piezoelectric properties. Ag and Mn as acceptor dopants substitute for Pb²⁺ and Zr⁴⁺/Ti⁴⁺, respectively, and this substitution influences lead as well as associated oxygen vacancies,

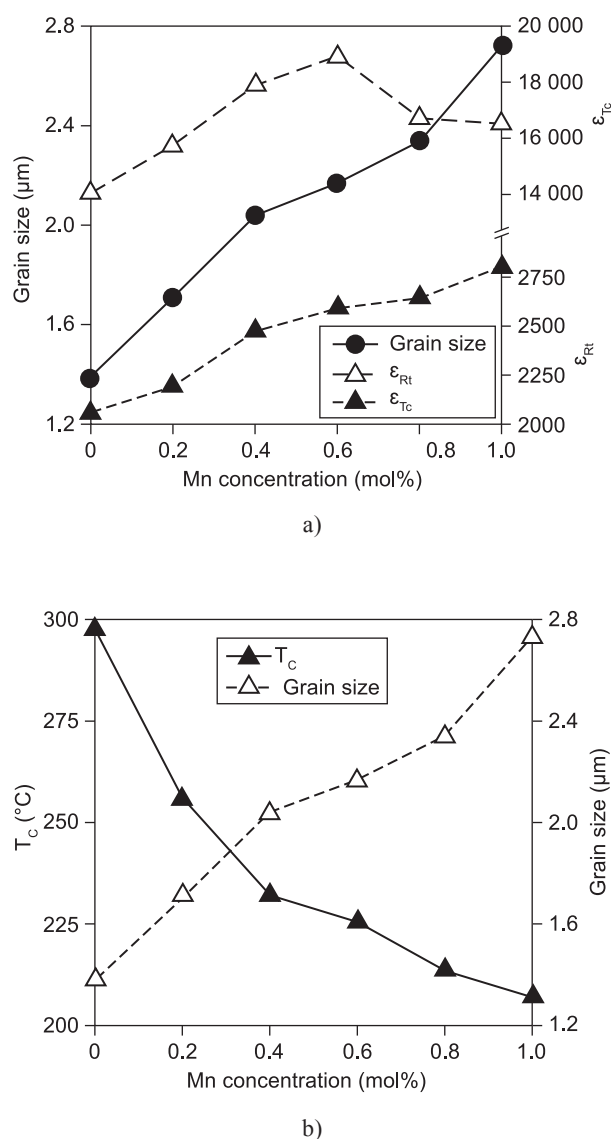


Figure 4. Dielectric properties, room temperature dielectric constant (ϵ_{RT}), dielectric maximum (ϵ_{TC}) and Curie temperature (T_c) vs. grain size of PLAZMT ceramics, respectively.

respectively, which may be attributed to the increase in the electromechanical behavior of PLAZMT ceramics. The effect of two acceptors (Ag and Mn) showed that Mn content helped in reducing/trapping the oxygen vacancies due to the reduction in the concentration of domain-stabilizing defect pairs while balancing the charge in the lattice. As a result, high piezoelectric planar coupling coefficient $k_p = 0.541$ and the piezoelectric charge coefficient $d_{33} = 548$ pC/N was observed in 1 mol.% Mn, respectively. Furthermore, the grain growth enhancement in the ceramics influenced domain orientation and thus, resulted in enhanced piezoelectric properties [29].

CONCLUSION

In conclusion, this paper reports on the effect of acceptor Ag occupying A-site reducing lead vacancies generated by the donor La^{3+} substitution and acceptor Mn occupying B-site reducing oxygen vacancies in PLZT perovskite. The dopants have influenced the microstructural development and resulted in excellent dielectric and piezoelectric properties. It is assumed that small quantities of Mn reduce or trap oxygen vacancies, reducing their mobility and therefore reducing the concentration of domain-stabilizing defect pairs. The addition of Ag tends to balance the vacancies caused by La, resulting in a homogeneous distribution in the PLZT perovskite structure. The oxygen, as well as lead, vacancies and the charge compensation play an important role in the compositional and microstructural homogenization of the PLAZMT perovskite. The optimum dielectric (ϵ_{RT}) and piezoelectric (d_{33} and k_p) properties enhanced proportionally with the grain growth while low T_c have been achieved in 1 mol.% Mn modified PLAZT ceramics which could be suitable for possible energy harvesting and electromechanical applications.

Acknowledgements

This work has been partially supported by Fondecyt, Chile. The authors would like to thank University of Concepcion, Chile and Andhra University, India for their collaboration and support extended. The authors would also like to thank Mr. Ranganathan, Mr. Krishnamurthy and Ms. C. N. Devi for their technical assistance and valuable suggestions extended during this work.

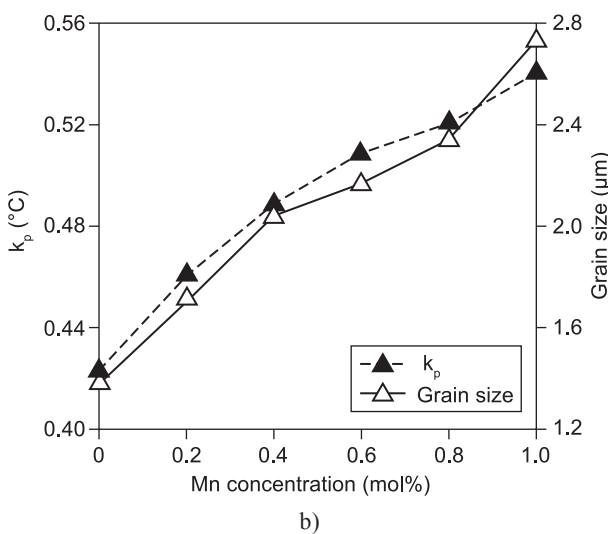
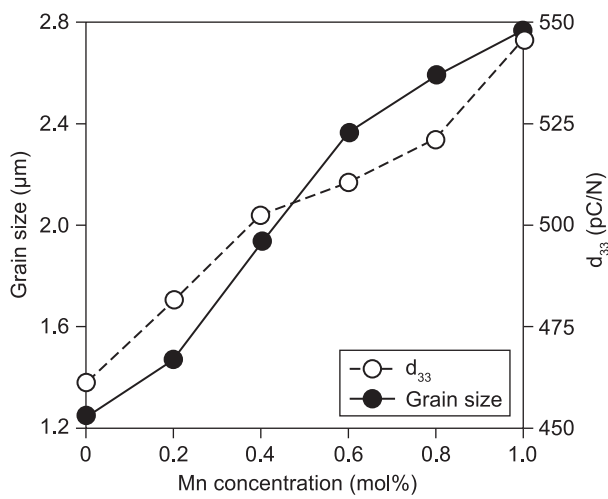


Figure 5. Piezoelectric properties (d_{33} and k_p) of PLAZMT ceramics, respectively.

References

- Jaffe B., Cook W.R., Jaffe H.: *Piezoelectric Ceramics*, Academic Press, London, U.K. (1971) pp. 140-160.
- Schulze W., Biggers J.: *Ferroelectrics* 9, 203 (1975).
- Maher G.H.: *J.Am.Ceram.Soc.* 66, 408 (1983).
- Weston T.B., Webster A.H., McNamara V.M.: *J.Am.Ceram.Soc.* 52, 253 (1969).
- Ramam K., Lopez M.: *Phys.Stat.Sol. A*, 203, 3852 (2006).
- Ramam K., Lopez M.: *J.Mater.Sci.: Mater.Electron.* (2007) doi 10.1007/s10854-007-9492-1.
- Lin D., Kwok K.W., Chan H.L.W.: *Materials Chemistry and Physics* 109, 455 (2008).
- Ramam K., Chandramouli K.: *Ceramics – Silikáty* 53, 189 (2009).
- Akashi T., Tsubouchi N., Takahashi M., Ohno T.: U.S. Patent 3461071 (1969).
- Uchida N., Ikeda T.: *Jpn.J.Appl.Phys.* 6, 1292 (1967).
- Yoon S. J., Joshi A., Uchino K.: *J.Am.Ceram.Soc.* 80, 1035 (1997).
- Suwannasiri T., Safari A.: *J.Am.Ceram.Soc.* 76, 3155

- (1983).
13. Kamiya T., Suzuki T., Tsurumi T., Daimon M.: *Jpn.J.Appl. Phys.* *31*, 3058 (1992).
14. Zhang Q., Whatmore R. W.: *J.Phys.D.Appl.Phys.* *34*, 2296 (2001).
15. Ramam K., Lopez M.: *J.Mater.Sci.: Mater.Electron.* *19*, 669 (2008).
16. Kanai H., Furukawa O., Nakamura S. I., Hayashi M., Yoshiki M., Yamashita Y.: *J.Am.Ceram.Soc.* *78*, 1173 (1995).
17. Hardtl K.H., Hennings D.: *J.Am.Ceram.Soc.* *55*, 230 (1972).
18. Koduri R., Lopez M.: *Eur.Phys.J.Appl.Phys.* *37*, 93 (2007).
19. Shannon R.D.: *Acta Cryst. A* *32*, 751 (1976).
20. Boucher E., Guyomar D., Lebrun L., Guiffard B., Grange G.: *J.Appl.Phys.* *92*, 5437 (2002).
21. Ikeda T.: *J.Physical.Soc.Jpn.* *14*, 168 (1959).
22. Zhang H., Li J.F., Zhang B.P.: *J.Am.Ceram.Soc.* *89*, 1300 (2006).
23. Kong L.B., Ma J., Zhu W., Tan O.K.: *Scripta Materialia* *44*, 345 (2001).
24. Kingon A.I., Clark J.B.: *J.Am.Ceram.Soc.* *66*, 256 (1983).
25. Hammer M., Hoffmann M.J.: *J.Am.Ceram.Soc.* *81*, 3277 (1998).
26. Zhang Q.M., Wang H., Kim N., Cross L.E.: *J.Appl.Phys.* *75*, 454 (1994).
27. Zhang Q., Whatmore R.W.: *J.Eur.Ceram.Soc.* *24*, 277 (2004).
28. Banerjee A., Bandyopadhyay A., Bose S.: *J.Am.Ceram.Soc.* *89*, 1594 (2006).
29. Guiffard B., Boucher E., Lebrun L., Guyomar D., Pleska E.: *Ferroelectrics* *313*, 135 (2004).
-